

The Conversion of CESR to Operate as the Test Accelerator, CEsRTA, Part 1: Overview

M.G.Billing

*Cornell University,
Ithaca, NY*

ABSTRACT: Cornell's electron/positron storage ring (CESR) was modified over a series of accelerator shutdowns beginning in May 2008, which substantially improves its capability for research and development for particle accelerators. CESR's energy span from 1.8 to 5.6 GeV with both electrons and positrons makes it ideal for the study of a wide spectrum of accelerator physics issues and instrumentation related to present light sources and future lepton damping rings. Additionally a number of these are also relevant for the beam physics of proton accelerators. This paper outlines the motivation, design and conversion of CESR to a test accelerator, CEsRTA, enhanced to study such subjects as low emittance tuning methods, electron cloud (EC) effects, intra-beam scattering, fast ion instabilities as well as general improvements to beam instrumentation. While the initial studies of CEsRTA focussed on questions related to the International Linear Collider (ILC) damping ring design, CEsRTA is a very flexible storage ring, capable of studying a wide range of accelerator physics and instrumentation questions. This paper contains the outline and the basis for a set of papers documenting the reconfiguration of the storage ring and the associated instrumentation required for the studies described above. Further details may be found in these papers.

KEYWORDS: Accelerator Subsystems and Technologies, Instrumentation for particle accelerators and storage rings, Beam-line instrumentation.

Contents

| | |
|---|-----------|
| 1. CEsrTA Collaboration | 1 |
| 2. Overview of CESRTA Program and CESR Modifications | 3 |
| 3. CESRTA Lattice and Layout | 4 |
| 3.1 Low Emittance Optics | 5 |
| 3.2 Energy Reach | 5 |
| 3.3 Grouped Control System Elements | 8 |
| 4. General Accelerator Modifications and Upgrades | 8 |
| 4.1 Overview | 8 |
| 4.2 Wiggler Straight Section Reconfiguration | 9 |
| 4.3 L3 Straight Section Reconfiguration | 12 |
| 4.4 Solenoid Windings | 12 |
| 4.5 Magnet System Controls Upgrades | 15 |
| 4.6 Alignment and Survey Upgrades | 17 |
| 5. Beam Instrumentation, Feedback Systems and Injection Controls | 19 |
| 5.1 Beam Instrumentation, Feedback System Upgrades | 19 |
| 5.2 Injection Control Upgrades | 20 |
| 6. Summary | 21 |

1. CEsrTA Collaboration

J.P. Alexander¹, F. Antoniou⁹, D. Asner⁷, R.P. Badman²⁶, J. Barley¹, L. Bartnik¹, M.G. Billing¹, L. Boon²⁴, K.R. Butler¹, J. Byrd²¹, S. Calatroni⁹, J.R. Calvey¹, B. Carlson¹⁴, D. Carmody⁸, F. Caspers⁹, C.M. Celata²¹, S.S. Chapman¹, J. Chu⁸, G.W. Codner¹, M. Comfort¹, C.C. Conolly¹, J.V. Conway¹, J.N. Corlett²¹, J.A. Crittenden¹, C. Cude¹⁷, M. Cunningham⁷, S. De Santis²¹, T. Demma¹⁸, C.A. Dennett¹, J.A. Dobbins¹, R. Dowd⁴, G.F. Dugan¹, N. Eggert¹, M. Ehrlichman¹, L. Fabrizio⁶, J. Flanagan¹⁹, E. Fontes¹, M.J. Forster¹, H. Fukuma¹⁹, M.A. Furman²¹, R.E. Gallagher¹, A.F. Garfinkel²⁴, M. Gasior⁹, S.W. Gray¹, S. Greenwald¹, D. Gonnella¹⁰, W. Guo⁵, K. Hammond¹⁵, L. Hales³⁰, K.C. Harkay³, D.L. Hartill¹, W. Hartung¹, Y. He¹, R. Helms¹, L. Hirshman¹, R.L. Holtzapple⁶, W.H. Hopkins¹, A. Jackson²¹, P. Jain¹⁹, H. Jin²³, R. Jones⁹, J. Jones¹¹, J. Kaminsky¹, K. Kanazawa¹⁹, J. Kandaswamy¹, S. Kato¹⁹, P. Kehayias²⁹, D. Kharakh²⁵, J-S. Kim¹, R. Kraft²¹, D.L. Kreinick¹, B. Kreis¹, K. Kubo¹⁹, J. Lanzoni¹, M. Lawson¹⁶, Z. Leong¹, Y. Li¹, H. Liu¹, X. Liu¹, J.A. Livezey¹, A. Lyndaker¹, R.J. Macek²⁰, J. Makita¹, M. McDonald¹, V. Medjidzade¹, R.E. Meller¹, T.P. Moore¹,

D.V. Munson²¹, J. Ng²⁵, K. Ohmi¹⁹, K. Oide¹⁹, N. Omcikus², T.I. O'Connell¹, M.A. Palmer¹, Y. Papaphilippou⁹, S.B. Peck¹, G. Penn²¹, D.P. Peterson¹, J. Pflingstner⁹, D.W. Plate²¹, M.T.F. Pivi²⁵, G.A. Ramirez¹, M. Randazzo⁶, A. Rawlins²¹, M.C. Rendina¹, P. Revesz¹, D.H. Rice¹, N.T. Rider¹, M.C. Ross¹³, D.L. Rubin¹, G. Rumolo⁹, D.C. Sagan¹, H. Sakai¹⁹, S. Santos¹, J. Savino¹, L. Schächter²⁷, H. Schmickler⁹, R.M. Schwartz¹, R. Seeley¹, J. Sexton¹, J. Shanks¹, K. Shibata¹⁹, J.P. Sikora¹, E.N. Smith¹, K.W. Smolenski¹, K.G. Sonnad¹, M. Stedinger¹, C.R. Strohman¹, Y. Suetsugu¹⁹, M. Taborelli⁹, H. Tajima¹⁹, C.Y. Tan¹³, A.B. Temnykh¹, D. Teytelman¹², M. Tigner¹, M. Tobiyama¹⁹, T. Ishibashi¹⁹, J. Urakawa¹⁹, J.T. Urban¹, S. Veitzer²⁸, M. Venturini²¹, S. Vishniakou¹, L. Wang²⁵, S. Wang¹, W. Whitney¹, E.L. Wilkinson²², T. Wilksen¹, H.A. Williams¹, A. Wolski¹¹, Y. Yariv¹, S.Y. Zhang⁵, M. Zisman²¹, R. Zwaska¹³

¹Cornell Laboratory for Accelerator-based Sciences and Education,
Cornell University, Ithaca, NY, 14850, U.S.A.

²American River College,
Sacramento, CA 95841, U.S.A.

³Argonne National Laboratory,
Argonne, IL 60439, U.S.A.

⁴Australian Synchrotron,
Clayton, 3168, Australia.

⁵Brookhaven National Laboratory,
Upton, NY 11973, U.S.A.

⁶California Polytechnic State University,
Physics Department, San Luis Obispo, CA 93407, U.S.A.

⁷Carleton University,
Department of Physics, Ottawa, Ontario, K1S 5B6, Canada

⁸Carnegie Mellon University,
Department of Physics, Pittsburgh, PA, 15389, U.S.A.

⁹CERN,
CH-1211 Genève 23, Switzerland

¹⁰Clarkson University,
Department of Physics, Potsdam, NY 13699, U.S.A.

¹¹Cockcroft Institute,
Warrington, Cheshire, U.K.

¹²Dimtel,
Inc., San Jose, CA 95124, U.S.A.

¹³Fermi National Accelerator Laboratory,
Batavia, IL 60510, U.S.A.

¹⁴Grove City College,
Physics Department, Grove City, PA 16127, U.S.A.

¹⁵Harvard University,
Department of Physics, Cambridge, MA 02138, U.S.A.

¹⁶Harvey Mudd College,
Department of Physics, Claremont, CA 91711, U.S.A.

- ¹⁷Indiana University,
Department of Physics, Bloomington, IN 47405, U.S.A.
- ¹⁸Istituto Nazionale di Fisica Nucleare - Laboratori Nazionali di Frascati,
00044 Frascati, Italy
- ¹⁹High Energy Accelerator Research Organization (KEK),
Tsukuba, Ibaraki 305-0801, Japan
- ²⁰Los Alamos National Laboratory,
Los Alamos, NM 87544, U.S.A.
- ²¹Lawrence Berkeley National Laboratory,
Berkeley, CA 94270, U.S.A.
- ²²Loyola University,
Department of Physics, Chicago, IL, 60626, U.S.A.
- ²³Postech,
Department of Physics, Pohang, Gyeongbuk 790-784, R.O.K.
- ²⁴Purdue University,
Department of Physics, West Lafayette, IN 47907, U.S.A.
- ²⁵SLAC National Accelerator Laboratory,
Menlo Park, CA 90425, U.S.A.
- ²⁶Syracuse University,
Department of Physics, Syracuse, NY 13244, U.S.A.
- ²⁷Technion-IIT,
Department of Electrical Engineering, Haifa, 32000, Israel
- ²⁸Tech-X Corporation,
Boulder, CO, 80303, U.S.A.
- ²⁹Tufts University,
Department of Physics and Astronomy, Medford, MA 02155, U.S.A.
- ³⁰University of Utah,
Department of Physics and Astronomy, Salt Lake City, UT 84112, U.S.A.

2. Overview of CESR-TA Program and CESR Modifications

The CESR-TA program was initially proposed to study accelerator physics questions related to the design of the electron and positron damping rings for the ILC accelerator complex. Several projects were determined to be appropriate for the CESR storage ring, which operates in the same ring with either electrons or positrons at energies comparable to those proposed for the damping rings. These goals group into five distinct categories with the associated references detailing some of the recent results of these studies:

- Developing techniques for tuning beams in storage rings for low vertical emittances.[26]
- Studying the dynamics for positron bunches within trains of bunches due to the growth of electron clouds along the trains.[5]
- Creating strategies to mitigate the effects of electron clouds on the positron bunches within trains.[11, 6, 10]

- Characterizing the effects of intra-beam scattering on single bunches.[16, 15, 8]
- Studying the effects of fast ion instabilities on the electron bunches within trains.[13, 12]

An additional overall goal for the CESR_{TA} program is to record and archive the data that is being acquired in order to make this available to accelerator physicists for testing future models of the phenomena that were studied as part of the program. As a consequence of this, the documentation of the storage ring's configuration, the accelerator environment in the experimental regions and the operation of the diagnostic instrumentation needs to be sufficiently complete for those, who would utilize this data in the future.

The conversion of CESR to permit the execution of the CESR_{TA} program required several extensive modifications. These included significant reconfiguring of CESR's accelerator optics by removing the CLEO high energy physics detector and its interaction region, moving six superconducting wigglers and reconfiguring the L3 straight section. There were also major vacuum system modifications to accommodate the changes in layout of the storage ring guide-field elements, to add electron cloud diagnostics and to prepare regions of the storage ring to accept beam pipes for the direct study of electron clouds (EC). A large variety of instrumentation was also developed to support new electron cloud diagnostics, to increase the capabilities of the beam stabilizing feedback systems and the beam position monitoring system, to develop new X-ray beam size diagnostics and to increase the ability for studying beam instabilities. The entire effort to reconfigure CESR and to install the new instrumentation took place over four separate accelerator down periods. This conversion process and the instruments developed for the CESR_{TA} program are described broadly in the following sections. These include the CESR_{TA} optics design, the accelerator lattice modifications and a general overview of instrumentation and controls upgrades.

This is the first of a four part series describing the conversion of CESR for the CESR_{TA} program. This paper describes an overview of the conversion project, including details on the accelerator lattice, magnets and controls, alignment and survey, injection controls and a broad overview of beam instrumentation. Part two documents the vacuum system modifications for the project. Required beam instrumentation upgrades are presented in part three. Part four describes the modification of superconducting wigglers to accommodate vacuum chambers containing retarding field analyzers for electron cloud spatial measurements and EC mitigations. More detailed discussion of the accelerator modifications and instrumentation may be found in the subsequent papers.

The initial phases of the CESR_{TA} program benefitted from the collaborative efforts of accelerator physicists and engineers from many laboratories throughout the world. As this paper provides an overview of the initial CESR_{TA} program and modification of the storage ring CESR to permit these studies, it seems appropriate to list our collaborators as co-authors to this paper to acknowledge our appreciation for their thoughts, suggestions and efforts.

3. CESR_{TA} Lattice and Layout

The CESR storage ring, outfitted with independently powered quadrupoles and sextupoles and 18 meters of superconducting damping wigglers is capable of operating with a very wide range of storage ring optics. Basic parameters for the storage ring are found in Table 1. The LINAC and synchrotron provide full energy injection of electron and positron beams. The storage ring

magnets allow operation over an energy range of 1.8 to 5.6 GeV. Multibunch feedback systems stabilize motion in all three planes for trains of bunches with bunch spacing of as short as 4 ns. The four single cell 500 MHz superconducting RF cavities operate over a range of gradients that enables investigations of bunch length dependencies. The complement of more than 100 steering correctors and 25 skew quad correctors is sufficient to eliminate relevant sources of vertical emittance dilution.

Table 1. Basic CESR Parameters

| Parameter | Value | Units |
|---|-----------------------|-----------|
| Ring Circumference | 768.438 | m |
| Circulation Period | 2.56 | μ sec |
| Operating Energy Range | 1.8 - 5.6 | GeV |
| RF System Frequency | 499.759 | MHz |
| Number of RF Buckets | 1281 | |
| Species | Electrons & Positrons | |
| Maximum Single Beam Current | 250 | mA |
| Any Combination of Bunches for 183 of 183 Buckets at a Spacing of | 14 | nsec |
| Any Combination of Bunches for First 600 Buckets at a Spacing of | 4 | nsec |

3.1 Low Emittance Optics

CESR achieves minimum emittance at a 2 GeV beam energy by employing superconducting damping wigglers, having a main period of 40 cm and operating at 1.9 T field strength.[24, 14, 23, 22] The wigglers reduce the radiation damping time by an order of magnitude and the horizontal emittance by a factor of 5 with respect to the wiggler off condition. The lattice functions are arranged so that there is zero horizontal dispersion in the wiggler straights. The relatively strong focusing and high horizontal tune minimizes the dispersion in the bend magnets and the resulting horizontal emittance. The lattice functions for the minimum emittance 2.085 GeV optics are shown in Figure 1. The independently-powered sextupoles are deployed to correct chromaticity in two families. Dynamic aperture is shown in Figure 2.

The damping wigglers are essential to achieving the low emittance in these optics. However, in the limit of a wiggler dominated ring, the minimum emittance is determined by the horizontal emittance generated within the wigglers themselves. With 12 wigglers that minimum is indeed obtained with a 1.9 T wiggler field. Higher wiggler fields will further reduce the damping time, but will increase the emittance due to the wiggler dispersion. The only way to further reduce the emittance with wigglers would be to increase the total length of wigglers, rather than increasing the wiggler field.

3.2 Energy Reach

We have designed and commissioned optics at 1.8, 2.085, 2.3 and 2.8 GeV, with all wigglers at 1.9 T

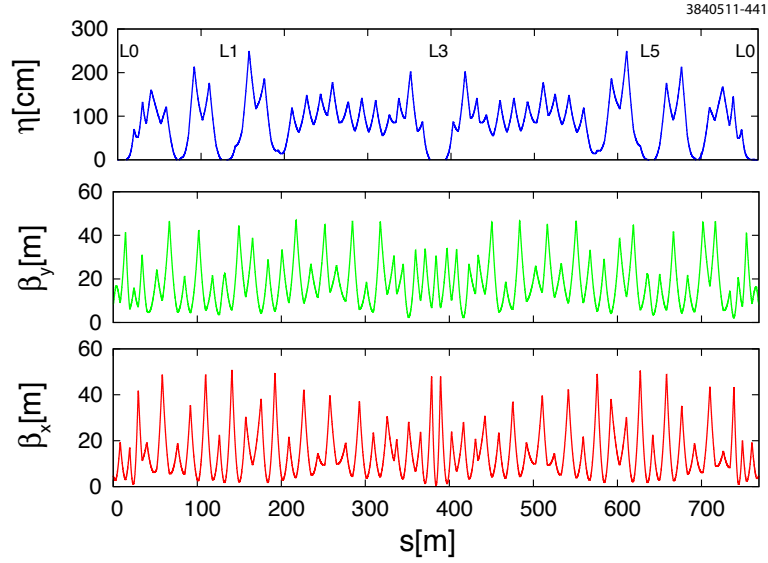


Figure 1. Design optics functions of low emittance ($\epsilon_x = 2.6$ nm-rad) lattice, with horizontal dispersion, η , at the top and the vertical and horizontal amplitude functions, β_y and β_x below. Regions of zero horizontal dispersion where damping wigglers are located are the L0 straight ($s = 0 \pm 10$ m where there are 6 wigglers) and L1 (126.7 m to 132.7 m, 3 wigglers) and L5 ($s = 635.8$ m to $s = 641.8$ m, 3 wigglers). L3 (384.2 \pm 9 m) is the experimental straight that includes the chicane for electron cloud studies and the in-situ SEY station. Retractable mirrors are used to reflect synchrotron radiation generated in the bends on either side of the L3 straight to the cave where optical instruments are located.

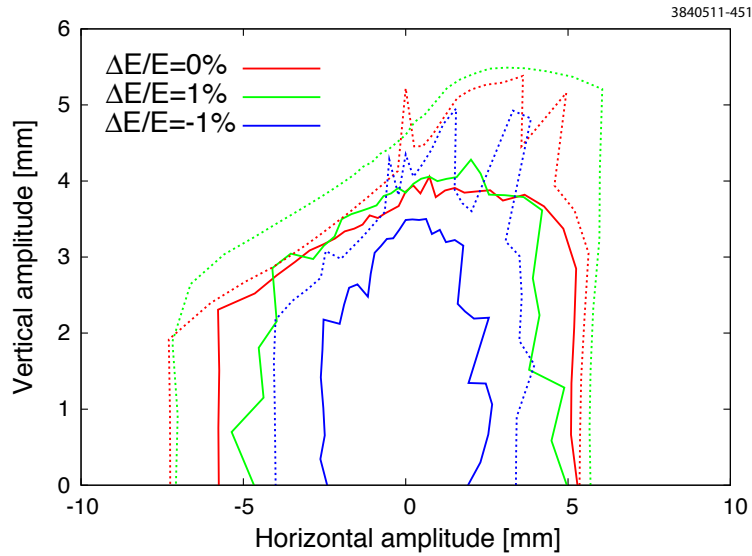


Figure 2. Simulation of the dynamic aperture for the low emittance lattice at 2.085 GeV. The solid curves are the maximum initial amplitude that survives 1000 turns at betatron tunes $Q_h = 14.595$, $Q_v = 9.63$, and synchrotron tune $Q_z = 0.0645$. The red, green and blue correspond to initial energy offsets of 0, $\pm 1\%$. The dashed lines are the maximum initial amplitude that survives for 20 turns and so approximate the physical aperture. Particles are lost at the real physical boundaries of the vacuum chamber.

field. At beam energy greater than 3 GeV, wiggler operation is limited to the those in the L0 straight. The vacuum chambers adjacent to the arc wigglers cannot sustain the synchrotron radiation power generated by these wigglers at high energies. Table 2 lists some of the CESR-TA lattice configurations that have been used for various measurements. The column, labelled Wiggler rad, refers to the fraction of the synchrotron radiation for the storage ring, which is produced by the wigglers. The rightmost column gives the fractional energy spread σ_E/E with the superconducting wigglers on and in optics roughly equivalent with the wigglers off. N.b. since the wigglers naturally provide vertical focusing, turning off wigglers requires significant changes in the quadrupole strengths near the wigglers. Although the wiggler off optics is not identical to the wiggler on optics, the energy spread variation caused by the wigglers being off is very nearly as specified in Table 2.

Table 2. Typical CESR-TA Lattice Configurations

| Lattice Name | Energy [GeV] | Emittance [nm-rad] | Wigglers @ 1.9 T | β_v at xBSM e^+ source | Wiggler rad [%] | σ_E/E (with/without) Wigglers [%] |
|-------------------------------|--------------|--------------------|------------------|--------------------------------|-----------------|--|
| CTA_1800MEV_ - XR40M_20110520 | 1.8 | 2.0 | 12 | 40 | 90 | (0.0767 / 0.0210) |
| CTA_2085MEV_ - XR20M_20091205 | 2.085 | 2.6 | 12 | 20 | 87 | (0.0813 / 0.0244) |
| CTA_2085MEV_ - XR40M_20091205 | 2.085 | 2.6 | 12 | 40 | 87 | (0.0813 / 0.0244) |
| CTA_2085MEV_ - 20090516 | 2.085 | 2.6 | 12 | 5.8 | 87 | (0.0813 / 0.0244) |
| CTA_2300MEV_ - XR40M_20110531 | 2.3 | 3.2 | 12 | 40 | 84 | (0.0843 / 0.0269) |
| CTA_3000MEV_ - Q0H_20090822 | 3.0 | 10.0 | 6 | 11.4 | 58 | (0.0841 / 0.0350) |
| CTA_4000MEV_ - 23NM_20090816 | 4.0 | 23 | 6 | 10.7 | 47 | (0.0888 / 0.0467) |
| CTA_5000MEV_ - 40NM_20090513 | 5.0 | 40 | 6 | 7.2 | 37 | (0.0903 / 0.0584) |
| CTA_5000MEV_ - 20090311 | 5.0 | 74 | 0 | 11.3 | 0 | (- / 0.0584) |

The use of superconducting wigglers also has an impact for the maximum beam current at high energy. The maximum wiggler power incident on the synchrotron radiation absorbers is limited to 40 kW for the six wigglers used at high energies. This limit was determined by synchrotron radiation calculations of the power deposited onto the absorbers with an opening angle of $1/\gamma$ at a fixed beam current. This information was processed using ANSYS to calculate a temperature and stress distribution in the absorbers. We have chosen to limit the beam current above 4 GeV beam energies to maintain a safety factor of at least three between the calculated maximum stress and the material's yield stress. The maximum operating currents for CESR at various operating energies

is given in Table 3. The very low current limits for electrons above 4 GeV with wigglers powered is due the lack of high power absorbers downstream of the L0 straight for the electron direction. More details on the superconducting wigglers may be found in Part 2, which describes the vacuum system.

Table 3. CESR-TA Operating Current Limits. These are the administrative limits placed on beam currents at different operating energies.

| Beam Energy [GeV] | Maximum Positron Total Current [mA] | Maximum Electron Total Current [mA] | Limited by Wiggler Power |
|----------------------|--|---|-----------------------------|
| 1.8 | 150 | 100 | no |
| 2.085 | 150 | 100 | no |
| 2.3 | 150 | 100 | no |
| 2.5 | 150 | 100 | no |
| 3.0 | 150 | 10 | yes |
| 4.0 | 100 | 3 | yes |
| 5.0 | 40 | 1 | yes |
| 5.0 | 240 | 240 | no |
| 5.3 | 240 | 240 | no |

3.3 Grouped Control System Elements

The flexibility of the CESR control system and the independent powering of all CESR magnets allow the possibility of creating grouped control elements (also called control knobs) for closed orbit, β , dispersion, and coupling bumps. We use orbit bumps to align the beam to position the source points for x-ray beam lines as required for the x-ray beam size monitor. In general, the beam size σ depends on emittance ϵ , amplitude function β , dispersion η , and energy spread δ , according to $\sigma = \sqrt{\epsilon\beta + (\eta^2\delta^2)}$. It is often convenient to be able to independently vary β , ϵ and dispersion to explore beam size monitor systematics and properties of the lattice. β -bumps are used to manipulate the beta function at the x-ray and visible light beam size monitor source points. A closed dispersion bump at the source of the horizontal beam size monitor allows a measurement of the contribution of the energy spread to the beam size. Closed coupling/dispersion bumps are used to vary vertical dispersion (and therefore vertical emittance) in a controlled way. We have developed code, which automatically computes coefficients and loads into the control system data base complete sets of orbit and coupling/dispersion bumps for each new lattice configuration. An example of the effect of such a coupling/dispersion bump is shown in Figure 3.

4. General Accelerator Modifications and Upgrades

4.1 Overview

The CESR storage ring, shown in figure 4, is capable of storing two counter-rotating beams with total currents up to 500 mA (or a single beam up to 250 mA) at a beam energy of 5.3 GeV. As

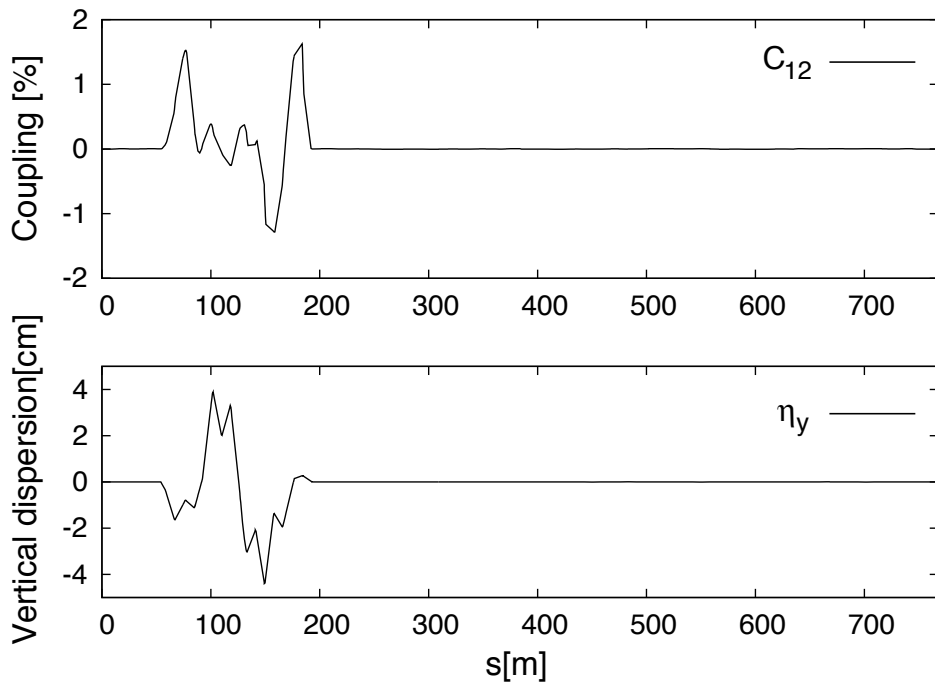


Figure 3. The closed coupling and vertical dispersion bump is generated with seven skew quads. The theoretical change to the vertical emittance (assuming that the unperturbed machine has zero coupling and zero vertical dispersion), is 25 pm-rad. The dispersion peak appears in the L1 region of the west arc wiggler straight. Bumps like this one are used to characterize the vertical beam size monitor and to vary emittance for investigation of intra-beam scattering, ion, and electron cloud effect.

shown in Table 1 the storage ring has a total length of 768.44 m, consisting of primarily bending magnets and quadrupoles in the arcs, two long straight sections, namely L0 (18.01 m in length) and L3 (17.94 m in length), and four medium length straights (namely, $L1, L5$, both 8.39 m in length and $L2, L4$, both 7.29 m in length).

4.2 Wiggler Straight Section Reconfiguration

CESR required extensive modifications for the straight section that contained the CLEO-c high energy physics (HEP) experimental detector[20]. During HEP operation this straight section was a micro-beta insert utilizing four superconducting quadrupoles and two permanent magnet final focus quadrupoles, all of which were oriented with approximately 4° tilts to compensate the CLEO solenoidal magnetic field. There was an additional pair of skew quadrupoles within the interaction region straight section to complete the solenoid compensation. During HEP operations the electron and positron bunches crossed at the interaction point with approximately a ± 2 mrad crossing angles, created by four horizontal separators placed symmetrically in the arcs of CESR. The layout of the HEP interaction region straight section is displayed in figure 5.

As a part of the CESR-c/CLEO-c HEP program twelve superconducting wigglers (SCWs) were installed in the southern one third of CESR[23]. For 2.1 GeV operation these wigglers provided 90% of the radiation damping in CESR and in their original arc locations could be used

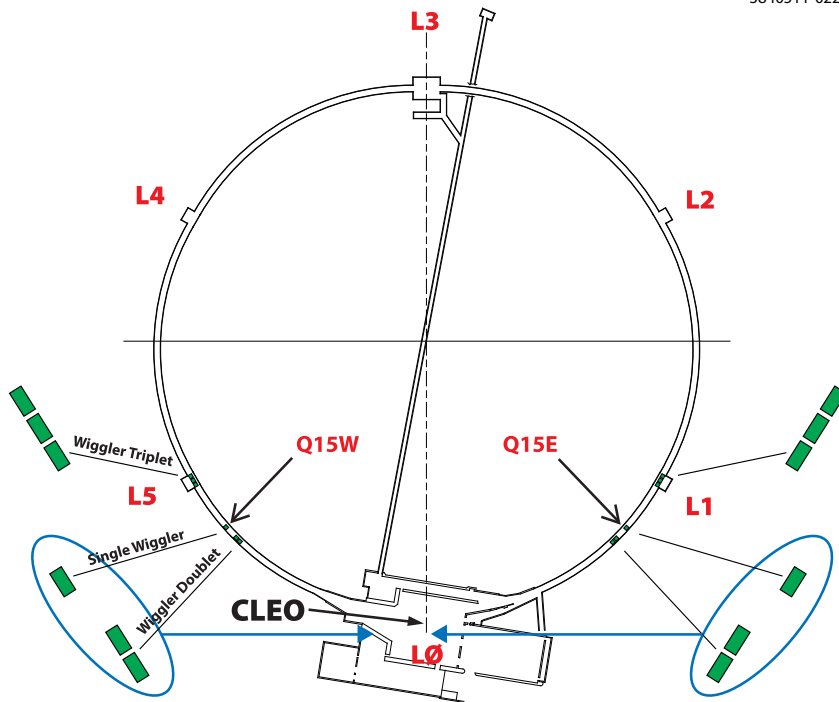


Figure 4. The reconfiguration of CESR accelerator components provided space in two long regions in L0 and L3, and two flexible short regions at Q15W and Q15E. Hardware for electron cloud studies was installed in these regions.

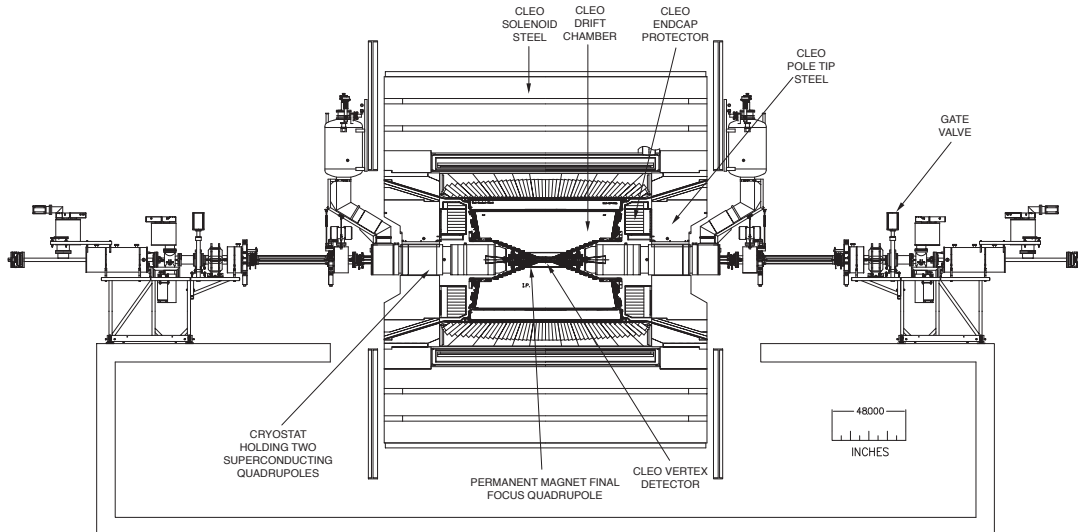


Figure 5. An elevation view of the CESR-c/CLEO-c interaction region before reconfiguration as the wiggler straight section for CESR-TA. The central section of the CLEO-c detector, the final focusing superconducting quadrupoles and the connecting vacuum chambers were removed during the CESR-TA installation.

for emittance control of the colliding beams. During CESR-c/CLEO-c HEP operations 6 of the 12 SCWs were installed as two triplet SCWs, located at two straight sections, namely L1 and L5, and the remaining 6 SCWs were in shorter straight sections between L0 and L1, and between L0 and L5. For the lowest emittance operation for CESRTA all twelve wigglers must be located in regions with zero dispersion. The CESRTA lattice provides for zero dispersion regions in the L0, L1 and L5 straight sections, which are shown in figure 4. Therefore six of the CESR-c wigglers were relocated to the CESR L0 straight, in the place of the CLEO drift chamber and endcaps. The other six wigglers, located in the L1 and L5 straight sections, remained in their original places.

3840511-040

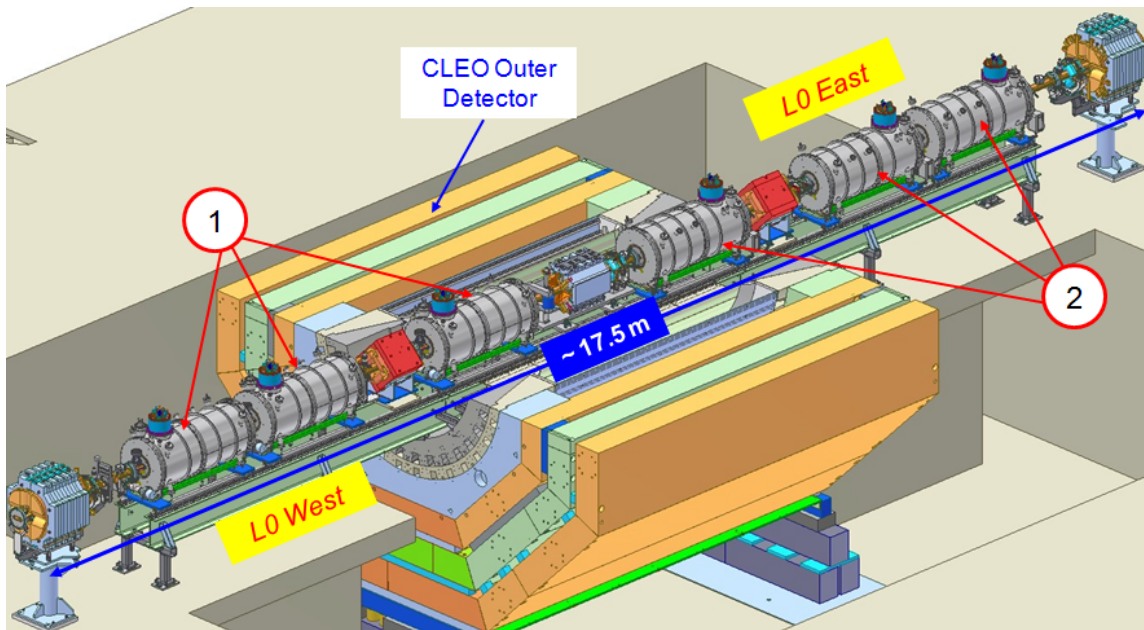


Figure 6. L0 center CESRTA EC experimental region, consists of (1) three retarding field analyzer-equipped SCWs and (2) three CESR-c SCWs. Many other EC diagnostics, such as retarding field analyzer (RFA) in the drifts, BPMs and TE-Wave buttons, are also implemented.

During the July 2008 shutdown, the central portion of the CLEO detector was decommissioned by removing the superconducting, normal conducting and permanent quadrupoles, the steering magnets for CESR, the CLEO endcap detectors, the vertex detector, the drift chamber and all of their associated cabling along with approximately 17 meters of vacuum chambers. All of these were located between the soft bend dipole magnets. A pair of bridging I-beams was installed through CLEO iron to support the quadrupole and steering magnets and the SCWs, which were positioned in the central portion of the L0 straight section. The six SCWs originally in the short straight sections between L0-L1 and L0-L5 were the wigglers relocated to the L0 long straight section as shown in figure 6. With the relocation all 12 SCWs are positioned in the long straight sections, in which the optics can be configured for zero dispersion, to produce the smallest possible beam emittances. Figure 6 shows the beam pipe, the conventional magnets and the six SCWs placed within the vacated CLEO detector's solenoid iron yoke. Figure 7 displays a view of the wiggler straight section.

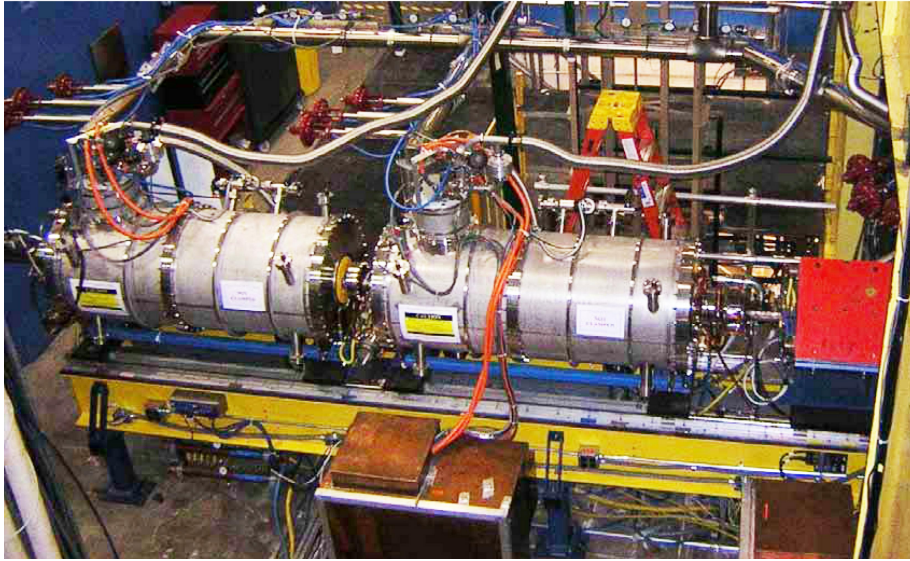


Figure 7. View of the wiggler straight section from the North on the East side of the wiggler straight section during the operation of CESR-TA. Two of the wiggler cryostats are visible as is a part of Q01E (orange magnet to the right of the cryostats.)

4.3 L3 Straight Section Reconfiguration

During CESR-c/CLEO-c HEP operations the L3 straight section (diametrically opposite to the CLEO-c detector's straight section) was configured to have a pair of electrostatic vertical separators, necessary to separate electron and positron bunches at the second horizontal angle crossing point for CESR, and an additional six quadrupoles forming a mini-beta insert. A schematic of the original optics layout for the central region of the L3 straight section is found in figure 8. To accommodate the planned experimental regions in this straight section, a major change to the accelerator optics was undertaken. After the removal of the pair of electrostatic vertical separators (outboard of the Q48W and Q48E quadrupoles), a long experimental straight section was established in the north region of CESR (L3). This 12-meter section, as shown in figure 9, is currently hosting many SLAC EC beam pipes for study and diagnostics, including a set of 4-dipole chicane magnets with beam pipes equipped with EC detectors, and an aluminum beam pipe with grooved interior. A pair of retractable synchrotron-light mirrors (highly polished beryllium) are set up for diagnostics and are used for beam profile measurements. Two in situ secondary electron emission yield (SEY) measurement systems were installed in the sector [18]. The SEY systems are equipped with load-locks, so SEY may be measured as a function of the beam dose for commonly used vacuum materials. Pictures of the experimental region are found in figure 10 and figure 11.

4.4 Solenoid Windings

Solenoid windings on drift sections of storage rings have been successfully employed to reduce

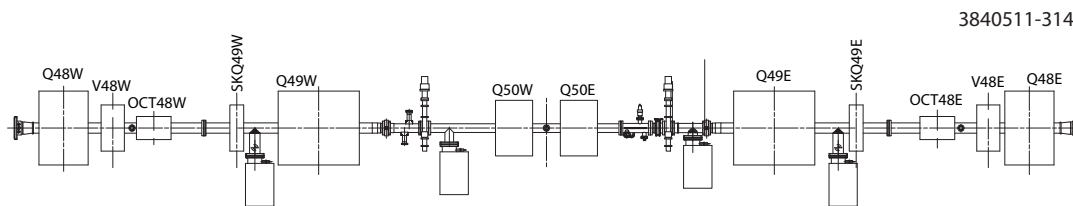


Figure 8. Schematic layout of the L3 optics between the vertical separators before reconfiguration for CESR TA operations.

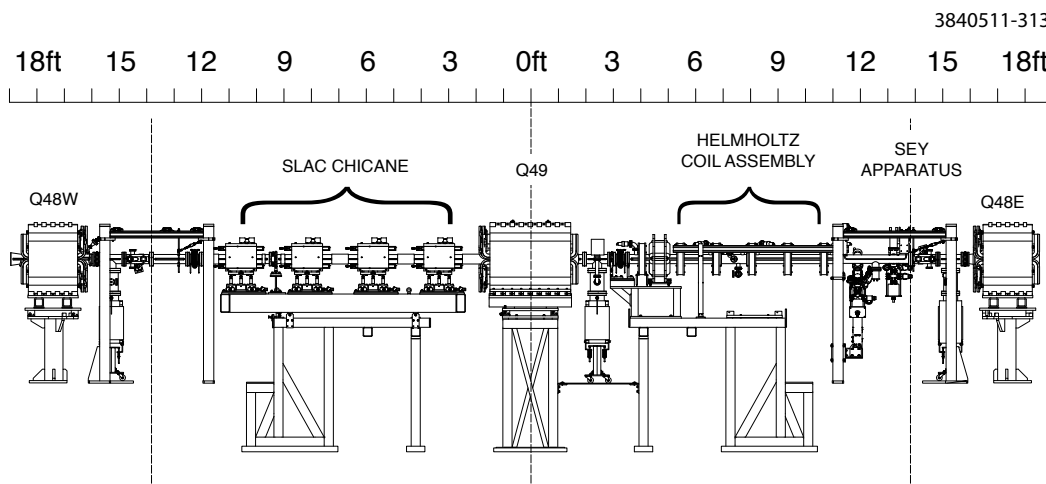


Figure 9. Schematic layout of the L3 experimental region. The experimental area includes the following vacuum chamber test regions: a chicane section, a region that has Helmholtz coils around the beam pipe to allow for chamber processing via bakeout etc., and an SEY apparatus with a lock-load mechanism to permit easy access for changing vacuum chamber wall surfaces.

the effect of electron clouds.[9, 17]. Although the total drift section length of CESR is only approximately 15% of the circumference and was not expected to play a major role in the electron cloud dynamical effects for the entire ring, elliptical solenoid windings have been added to cover approximately 80% of this drift length. The windings were wrapped directly on the CESR vacuum chamber after a thin Kapton insulating layer was added around the radial outside of the chamber to effectively enlarge the 3 mm radius corners above and below the water cooling channel to prevent the radii of curvature for the solenoid cable becoming too small at these two corners. In a few sections of the storage ring the beam pipe is circular so in these places the windings are cylindrical solenoids. In the experimental region in the L3 straight section, several Helmholtz coils were employed to allow better access to the vacuum chamber; the spacing between the coils was set to have the longitudinal field for these coils approximately the same as in the standard solenoid windings. The cable, employed for the windings wrapped directly on the beam pipe, is radiation hard number 10 (AWC) gauge insulated wire, which is wound in a single close-packed single layer. A few examples of the Helmholtz coils and solenoid windings maybe seen in figure 11, figure 12 and figure 13. Windings in adjacent drift sections are clustered together and connected in series to one switching DC power supply, where an effort has been made to reduce the net longitudinal magnetic

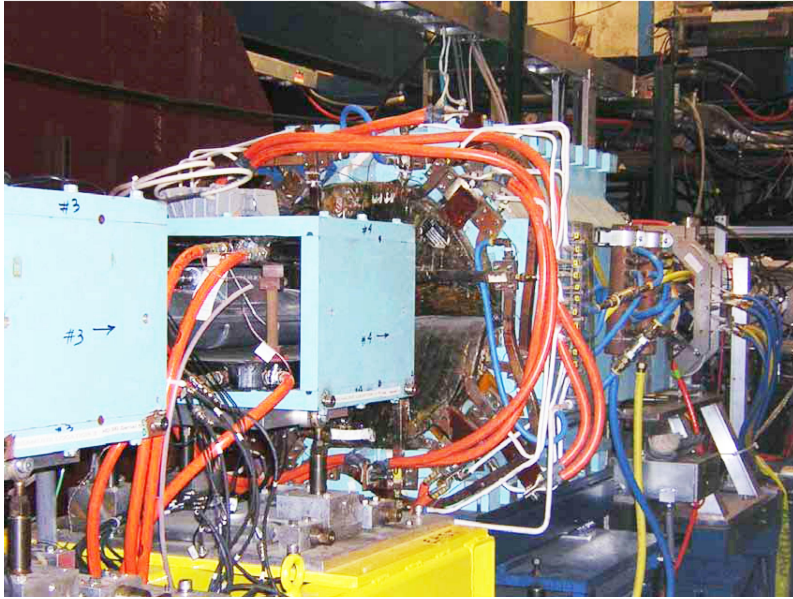


Figure 10. View of the L3 experimental region looking to the East and showing two of the chicane magnets in the foreground followed by Q49.

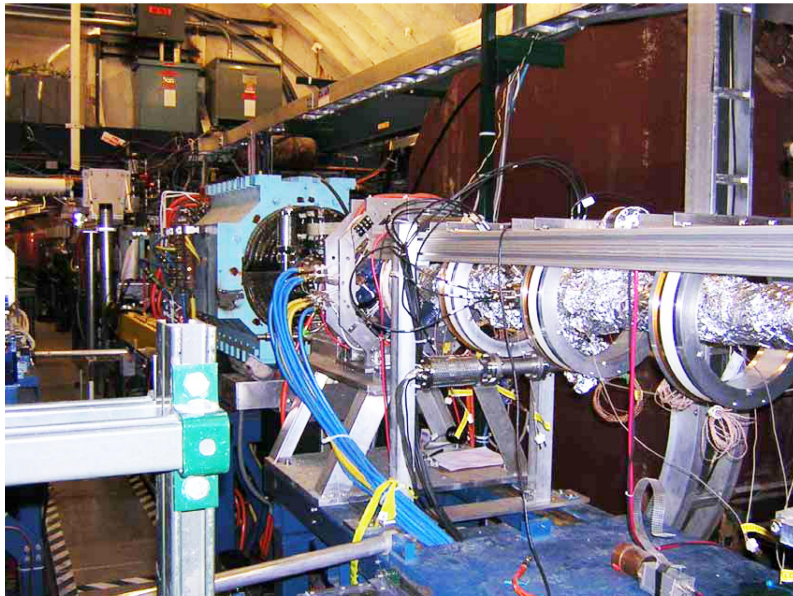


Figure 11. L3 experimental region viewing Q49 from the East and having the Helmholtz coils around the beam pipe for studies of Electron Cloud suppression. The picture also shows the Helmholtz coils surrounding the vacuum chamber as it is being prepared for a bakeout.

field by arranging the polarity of the windings to roughly balance the number of turns which have the current flowing clockwise around the vacuum chamber with those where it is flowing counter-clockwise. This reduces the local horizontal-vertical coupling of the beam's motion caused by each

supply powering an individual cluster of solenoid windings.

The power supplies are generally unipolar 25 A switching DC power supplies operating off of the common 65 VDC ring magnet power supply bus. The power supplies function with the same control system hardware and software as the CESR steering power supplies. The winding resistance for the adjacent drift sections, as clustered together and connected in series, is less than 2.5Ω , being low enough to allow the full 25 A of current. In two instances where the solenoid windings surround the shielded pickups, 100 A bipolar supplies were installed (and limited to ± 25 A operation) to permit sweeping the solenoid field over both polarities for the shielded pickup measurements.

During installation the polarities of the windings for all of the separate drift sections was verified to have the required alternation needed to reduce the horizontal-vertical coupling effects. After installation the magnitude of the longitudinal magnetic field was measured to be approximately 40 G for a 25 A excitation in the standard CESR beam pipe windings. A single positron bunch in 2.1 GeV conditions was used to check the coupling error caused by each of the 16 clusters of windings. After adjusting the minimum tune split on the coupling resonance to be less than 0.0002, the change in the global coupling of the bunch was measured when all of the solenoid power supplies were excited to their full currents. With all solenoid power supplies at full current the accelerator minimum tune split on the coupling resonance was 0.0027. Since the solenoids were installed primarily to study their effect on the cloud's density, they are usually powered only during mitigation or shielded pickup measurements.

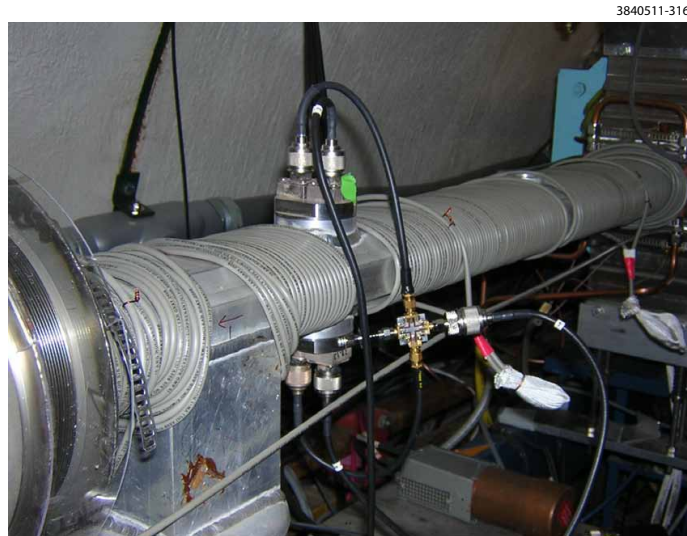


Figure 12. View of solenoid windings on one typical arc vacuum chamber.

4.5 Magnet System Controls Upgrades

The conversion of CESR to a test accelerator to study low emittance beams and the effects of electron clouds has required significant additions or changes to the accelerator controls. The first set of changes is obvious from the preceding sections: the reconfiguration of the magnet controls for the conventional accelerator magnet system. The change to CESR's optics and steering controls

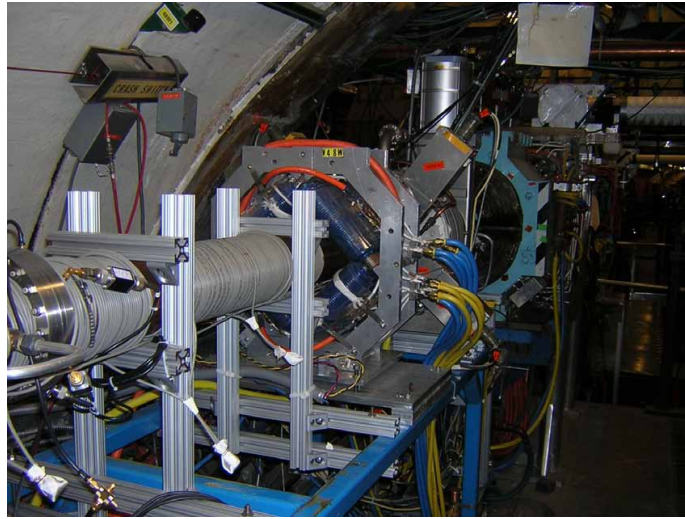


Figure 13. View of solenoidal field windings on the L3 straight section vacuum chambers.

required the removal, installation, reconfiguration or re-cabling of 48 separate magnets in the ring for the wiggler and L0 straight sections. The elements, which were installed for CESR TA operations, are summarized in Table 4.

In addition to the aforementioned magnet supplies several other types of magnets were either moved or installed around the ring for CESR TA use. These include the wigglers that were moved into the wiggler straight section from their location in the storage ring's arcs between L0 and either L1 or L5 straight sections. Figure 14 presents a view of some of the wigglers in the wiggler straight section and figure 15 shows one of the power supply control racks. The wiggler straight section's construction required the relocation of six wigglers, their cryogenic controls and power supplies. The rack of control electronics includes a number of control and monitoring functions. The first is the "Ready Chain" for the protection of the magnets and power supplies, which requires elements such as the primary power, water and cryogenic cooling, the quench protection be enabled and heat sink temperature monitor be below their trip levels, in order for the power supplies to turn on. The power supplies are a 300 A-3.3 V wiggler main supply and an 8 A-15 V steering trim supply. There is also monitoring circuitry including 16 channels of cryogenic temperature readouts, 20 channels of voltage, current, cryogen level and pressure sensor slow readouts, 8 channels of fast quench protection readouts.

The chicane magnets and their power supplies in the L3 experimental area are on loan from SLAC during the CESR TA experimental run. The chicane consists of four dipole magnets wired with field polarities of +, -, -, and +. They are powered with two DC supplies having a total of 235 A at 56 V. The system is current regulated using a Danfysic current transformer connected to a modified CESR 16-bit unipolar regulator card, which provides a 10 V maximum control signal to the main DC power supplies. The integrator in the lead-lag circuit of the regulation loop is adjusted to compensate the magnets' time constant of 0.074 sec. The modified CESR 16 bit magnet controller card was chosen as it has a common connection to the CESR magnet clock, which allows for coordinated excitation of the chicane magnets with other CESR magnets. This permits

Table 4. Listing of standard CESR accelerator elements, which were installed, re-cabled or reconfigured for CESRTA operation.

| Name(s) of CESRTA Element | Type of Power Supply | Maximum Current | Maximum Voltage | Number of PSs |
|---------------------------|---|-----------------|-----------------|---------------|
| Q00W | Linear Pass-bank Regulated | 250 A | 28 V | 1 |
| Q01W, Q01E | Precision Chopper Switching Regulator | 80 A | 55 V | 2 |
| Q02W (16T), Q02E (16T) | Precision Regulated EMI PS | 1000 A | 20 V | 2 |
| Q48W (6T PS) Q48E (6T PS) | In series with dipole magnets - Transrex PS's | 700 A | 300 V | 1 |
| Q48W (22T), Q48E (22T) | Linear Pass-bank Regulated | 250 A | 28 V | 2 |
| Q49W (22T) | Precision Regulated EMI PS | 1000 A | 20 V | 1 |
| H01W | Bipolar Chopper Switching Regulator | ± 12.5 A | ± 55 V | 1 |
| V01E | Bipolar Chopper Switching Regulator | ± 12.5 A | ± 55 V | 1 |
| V02W, V02E | Bipolar Chopper Switching Regulator | ± 12.5 A | ± 55 V | 2 |
| SQ01E | Bipolar Chopper Switching Regulator | ± 12.5 A | ± 55 V | 1 |
| SQ02W, SQ02E | Bipolar Chopper Switching Regulator | ± 12.5 A | ± 55 V | 2 |
| H49E | Bipolar Chopper Switching Regulator | ± 12.5 A | ± 55 V | 1 |
| V49E | Bipolar Chopper Switching Regulator | ± 12.5 A | ± 55 V | 1 |
| V48W, V48E | Bipolar Chopper Switching Regulator | ± 12.5 A | ± 55 V | 2 |
| SQ48W, SQ48E | Bipolar Chopper Switching Regulator | ± 12.5 A | ± 55 V | 2 |

the simultaneous scaling of the current command to the chicane magnets with any other CESR magnet, e.g. to have coordinated scaling of the chicane field with other CESR steering elements.

4.6 Alignment and Survey Upgrades

Meeting the more stringent alignment tolerances specified by the CESRTA project required an up-

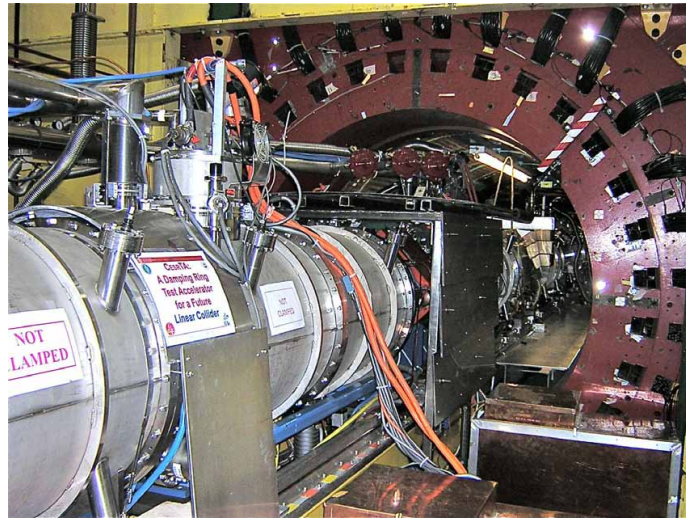


Figure 14. Wigglers in the wiggler straight section with their controls. The picture shows a view looking into the former CLEO detector with two of the three wigglers displayed to the left and the cabling of rightmost of these two in the center of the picture.

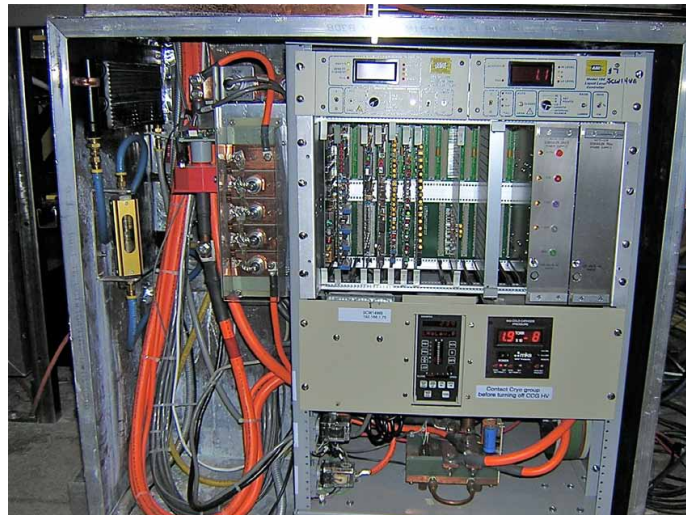


Figure 15. This picture presents a view of the wiggler control rack, which contains all of the controls, monitoring and the power supplies for the wiggler and its steering trim coils.

grade to both the survey monument hardware and the survey equipment. All upgrade changes were essentially determined by the conversion of main surveying instrument from a Leica TDM5005 total station to an API Tracker III laser tracker with interferometer. The laser tracker requires monument hardware, which would accept the 1.5 inch spherically mounted reflectors (SMR's), and also supporting instruments, which could accurately measure the gravity based heights of the reference target. These were necessary, since at the time of purchase no laser tracker had an integrated high precision gravity based level and compensator. Thus, a Leica DNA03 digital level and its

measurement staffs completed the survey instrument upgrade.

After some study of the available hardware, and a training and observation trip to Lawrence Berkeley National Laboratory's Advanced Light Source we chose to use Hubb's Machine and Manufacturing, Inc. drift nests and floor targets. Tack welding the drift nests onto Uni-Strut gussets resulted in cost effective and very stable wall targets, which attached to our existing Uni-Strut ribs in the tunnel walls. The floor targets were permanently epoxied into holes drilled in the concrete floor of the tunnel with a core drill. The o-rings covers and stainless steel construction of the floor targets provided good protection against water infiltration and corrosion. Triplets of two wall targets (on inside and outside tunnel walls) and one floor target (near the center of the tunnel floor) spaced at approximately 8 to 10 meters apart provided the necessary geometry to meet the alignment tolerances.

With the utilization of the new survey instruments significant improvements were made in the positioning of accelerator components. The initial surveys yielded RMS spreads of $206 \mu\text{rad}$ for the dipole tilts, $227 \mu\text{rad}$ for the quadrupole tilts and $193 \mu\text{m}$ for the quadrupole vertical offsets. After survey and re-alignment the RMS spreads were reduced to $130 \mu\text{rad}$ for the dipole tilts, $50 \mu\text{rad}$ for the quadrupole tilts and $27 \mu\text{m}$ for the quadrupole vertical offsets.[25] With these improvements in the positioning of the accelerator components vertical emittances of 10 pm were achieved.[26]

5. Overview of Beam Instrumentation, Feedback Systems and Injection Controls

5.1 Beam Instrumentation, Feedback System Upgrades

The undertaking of the CESR-TA project required the development or upgrading of several accelerator operating systems. The significant improvements to beam instrumentation are summarized as follows:

- A major upgrade to the beam position monitor system, which replaced an older relay-based position monitor system with individual readout modules for each monitor capable of turn-by-turn and bunch-by-bunch trajectory measurements for bunches spaced as closely as 4 ns [21].
- The installation of positron and electron x-ray vertical beam size monitors designed for turn-by-turn and bunch-by-bunch beam size measurements for 4 ns spaced bunches [27].
- Implementation of positron and electron visible-light monitors to measure the horizontal beam size, including the addition of optical elements to allow streak camera measurements of both electron and positron bunches [1, 2].
- Development of software to extract bunch-by-bunch tunes utilizing the new modules for the beam position monitors and a second method, which employed video gating of signal from a few beam position monitors from the older relay system [4, 7].
- An upgrade for the tune tracker, which is phase locked to the betatron tunes of a bunch. This device allows the measurement of the betatron phase advance and the horizontal-to-vertical coupling of CESR permitting their correction [19].

- Installation of a new beam-stabilizing feedback system, which damps 4 ns-spaced bunches for horizontal, vertical and longitudinal motion, in addition to the existing 14 ns feedback system [3].

This instrumentation is described in further detail in companion papers. Additionally hardware and software infrastructure was created for X-ray beam size monitors, the CESR beam position monitors and electron cloud detectors. This included the installation of modest bandwidth and wide bandwidth interfaces to all of these detectors. It also included the software interfaces and data structures to operate this hardware and to communicate their data to the data acquisition software.

5.2 Injection Control Upgrades

During most of its operations, CESR stored beams with bunches spaced in multiples of 14 ns. As a result, all of the current monitoring instrumentation was configured for 14 ns as the minimum spacing. To accommodate the multiple of 4 ns-spaced bunches for CESR-TA, a new current monitor was developed. This current monitor utilizes a standard BPM button position monitor connected to one of the new CESR beam position monitor modules, which was programmed specifically to return a constant times the sum of the button signals as the bunch current. This monitor is capable of measuring all stored bunches with a minimum of a 4 ns-spacing over the desired bunch current range with an update rate of 3 Hz.

The current monitor is an integral component utilized by the injection software. This program reads the current monitor to obtain the charge in each of the bunches, it then turns on the appropriate triggers to the gun pulser in order to accelerate a set of bunches to fill the storage ring. Substantial revisions were needed for this software to accommodate more general timing patterns for the stored bunches in CESR. This is the case since the lowest common harmonic frequency shared by the LINAC injector RF, the LINAC RF accelerator cavities, the synchrotron accelerator cavities and CESR's RF system is 71.4 MHz, equaling a bunch spacing of 14 ns. Injecting any multiple of 14 ns-spaced bunches only requires turning on triggers for the gun pulser at the correct time and the bunches can be accelerated and be stored in CESR with no change of any RF system phase. However, injecting 4 ns-spaced bunches requires an additional shift of all of the injector's RF phases for bunches to line up with proper CESR RF buckets. The upgraded injection software employed a new operator interface to specify which RF buckets were to be filled in CESR while accomplishing the required triggering for the gun pulser and injector RF phase shifts to store these bunches.

The injection software had new protection algorithms added, which limits the total current that can be stored in CESR. This is necessary for several reasons. When the superconducting wigglers are powered, software interlocks limit the total beam current to prevent their X-ray flux from damaging the downstream vacuum chamber walls. When the xBSM's optics chip is inserted in the X-ray beam, both software and hardware interlocks limit the total stored beam current. Also as a failsafe mechanism for communications failure of the bunch-by-bunch current monitor, the injection triggers are disabled whenever the sum of the bunch currents significantly disagrees with the DC current monitor.

6. Summary

Major changes were required to modify the CESR storage ring to support the creation of CESR-TA, a test accelerator configured to study accelerator physics issues over a wide spectrum of accelerator physics effects and instrumentation related to present light sources and future lepton damping rings. The modifications were undertaken during four separate accelerator down periods ranging in length from one to four months with these occurring between CESR operating runs for the x-ray science program for CHESS. When operating for the CESR-TA program, CESR's optics and instrumentation has been optimized for the study of low emittance tuning methods, electron cloud effects, inter-beam scattering, fast ion instabilities as well as general improvements to beam instrumentation.

References

- [1] J. P. Alexander, A. Chatterjee, C. Conolly, E. Edwards, M. P. Ehrlichman, J. W. Flanagan, E. Fontes, B. K. Heltsley, W. Hopkins, A. Lyndaker, D. P. Peterson, N. T. Rider, D. L. Rubin, R. Seeley, and J. Shanks, *Design and performance of coded aperture optical elements for the cesr-ta x-ray beam size monitor*, Nucl. Instrum. Methods Phys. Res. **A767** (2014), 467–474.
- [2] J. P. Alexander, A. Chatterjee, C. Conolly, E. Edwards, M. P. Ehrlichman, E. Fontes, B. K. Heltsley, W. Hopkins, A. Lyndaker, D. P. Peterson, N. T. Rider, D. L. Rubin, J. Savino, R. Seeley, J. Shanks, and J. W. Flanagan, *Vertical beam size measurement in the cesr-ta e^+e^- storage ring using x-rays from synchrotron radiation*, Nucl. Instrum. Methods Phys. Res. **A748** (2014), 96–125.
- [3] M. Billing, G. Codner, D. Hartill, R. Meller, J. Sikora, and V. Vescherevich, *Performance of the beam stabilizing feedback systems at cesr*, Proceedings of the 2001 Particle Accelerator Conference, Chicago, IL (P. Lucas and S. Webber, eds.), IEEE, 2001, pp. 1243–1245.
- [4] M. Billing, G. Dugan, R. Meller, M. Palmer, G. Ramirez, J. Sikora, H. Williams, and R. Holtzapple, *Techniques for observing beam dynamical effects caused by the presence of electron clouds*, Proceedings of E-CLOUD 2010: 49th ICFA Advanced Beam Dynamics Workshop on Electron Cloud Physics, Ithaca, NY (Ithaca, NY) (Karl Smolenski, ed.), Cornell University, 2013, pp. 108–117.
- [5] M. G. Billing, L. Y. Bartnik, K. D. Butler, G. Dugan, M. J. Forster, G. A. Ramirez, N. T. Rider, K. Sonnad, H. A. Williams, R. L. Holtzapple, K. McArdle, M. Miller, M. Totten, and J. W. Flanagan, *Recent results for the dependence of beam instabilities caused by electron clouds at cesr-ta due to variations in bunch spacing and chromaticity*, IPAC2014: Proceedings of the 5th International Particle Accelerator Conference, Dresden, Germany (Geneva, Switzerland) (Christine Petit-Jean-Genaz, Gianluigi Arduini, Peter Michel, and Volker R. W. Schaa, eds.), JACoW, 2014, pp. 1721–1723.
- [6] M. G. Billing, J. Conway, E. E. Cowan, J. A. Crittenden, W. Hartung, J. Lanzoni, Y. Li, C. S. Shill, J. P. Sikora, and K. G. Sonnad, *Measurement of electron trapping in the cesr storage ring*, Tech. Report arXiv:1309.2625, Cornell University Library, Ithaca, New York, December 2014, submitted to Phys. Rev. ST Accel. Beams.
- [7] M. G. Billing, G. Dugan, R. Meller, M. Palmer, M. Rendina, N. Rider, J. Sikora, C. Strohman, and R. L. Holtzapple, *Techniques for observation of beam dynamics in the presence of an electron cloud*, Proceedings of the 2010 International Particle Accelerator Conference, Kyoto, Japan, ACFA, 2010, pp. 1197–1199.
- [8] K. J. Blaser, A. Chatterjee, M. P. Ehrlichman, W. Hartung, B. Heltsley, D. P. Peterson, D. Rubin, D. Sagan, J. P. Shanks, and S. T. Wang, *Measurement of beam size in intrabeam scattering dominated*

- beams at various energies at cesrta*, IPAC2014: Proceedings of the 5th International Particle Accelerator Conference, Dresden, Germany (Geneva, Switzerland) (Christine Petit-Jean-Genaz, Gianluigi Arduini, Peter Michel, and Volker R. W. Schaa, eds.), JACoW, 2014, pp. 1635–1637.
- [9] Y. Cai, M. Pivi, and M. A. Furman, *Buildup of electron cloud in the pep-ii particle accelerator in the presence of a solenoid field and with different bunch pattern*, Phys. Rev. ST Accel. Beams **7** (2004).
- [10] J. R. Calvey, W. Hartung, Y. Li, J. A. Livezey, J. Makita, M. A. Palmer, and D. Rubin, *Comparison of electron cloud mitigating coatings using retarding field analyzers*, Nucl. Instrum. Methods Phys. Res. **A760** (2014), 86–97.
- [11] ———, *Measurements of electron cloud growth and mitigation in dipole, quadrupole, and wiggler magnets*, Nucl. Instrum. Methods Phys. Res. **A770** (2015), 141–154.
- [12] A. Chatterjee, K. Blaser, M. Ehrlichman, D. Rubin, and J. Shanks, *Fast ion instability at cesr-ta*, IPAC2014: Proceedings of the 5th International Particle Accelerator Conference, Dresden, Germany (Geneva, Switzerland) (Christine Petit-Jean-Genaz, Gianluigi Arduini, Peter Michel, and Volker R. W. Schaa, eds.), JACoW, 2014, pp. 1638–1640.
- [13] A. Chatterjee, K. Blaser, W. Hartung, D. Rubin, and S. T. Wang, *Fast ion instability at cesr-ta*, submitted to Phys. Rev. ST Accel. Beams in September 2014.
- [14] J. A. Crittenden, A. Mikhailichenko, and A. Temnykh, *Design considerations for the cesr-c wiggler magnets*, Proceedings of the 2003 Particle Accelerator Conference, Portland, OR (Joe Chew, Peter Lucas, and Sara Webber, eds.), IEEE, 2003, pp. 1954–1956.
- [15] M. P. Ehrlichman, A. Chatterjee, W. Hartung, B. Heltsley, D. P. Peterson, N. Rider, D. Rubin, D. Sagan, J. P. Shanks, and S. T. Wang, *Measurement and compensation of horizontal crabbing at the cornell electron storage ring test accelerator*, Phys. Rev. ST Accel. Beams **17** (2014).
- [16] M. P. Ehrlichman, W. Hartung, B. Heltsley, D. P. Peterson, N. Rider, D. Rubin, D. Sagan, J. Shanks, S. T. Wang, R. Campbell, and R. Holtzapple, *Intrabeam scattering studies at the cornell electron storage ring test accelerator*, Phys. Rev. ST Accel. Beams **16** (2013).
- [17] Hitoshi Fukuma, *Electron cloud instability in kekb and superkekb*, ICFA Beam Dynamics Newsletter (M. E. Biagini, ed.), no. No. 48, International Committee on Future Accelerators, April 2009, pp. 112–118.
- [18] W. H. Hartung, D. M. Asner, J. V. Conway, C. A. Dennett, S. Greenwald, J.-S. Kim, Y. Li, T. P. Moore, V. Omanovic, M. A. Palmer, and C. R. Strohmman, *In-situ measurements of the secondary electron yield in an accelerator environment: Instrumentation and methods*, Tech. Report arXiv:1407.0772, Cornell University Library, Ithaca, New York, December 2014, accepted for publication in Nucl. Instrum. Methods. Phys. Res. A.
- [19] R. E. Meller and M. A. Palmer, *Digital tune tracker for cesr*, Proceedings of the 2011 Particle Accelerator Conference, New York, NY, IEEE, 2011, pp. 504–506.
- [20] M. A. Palmer, J. Alexander, M. Billing, J. Calvey, S. Chapman, G. Codner, C. Conolly, J. Crittenden, J. Dobbins, G. Dugan, E. Fontes, M. Forster, R. Gallagher, S. Gray, S. Greenwald, D. Hartill, W. Hopkins, J. Kandaswamy, D. Kreinick, Y. Li, X. Liu, J. Livezey, A. Lyndaker, V. Medjidzade, R. Meller, S. Peck, D. Peterson, M. Rendina, P. Revesz, D. Rice, N. Rider, D. Rubin, D. Sagan, J. Savino, R. Seeley, J. Sexton, J. Shanks, J. Sikora, K. Smolenski, C. Strohmman, A. Temnykh, M. Tigner, W. Whitney, H. Williams, S. Vishniakou, T. Wilksen, K. Harkay, R. Holtzapple, E. Smith, J. Jones, Y. He, M. Ross, C. Y. Tan, R. Zwaska, J. Flanagan, P. Jain, K. Kanazawa, K. Ohmi, H. Sakai, K. Shibata, Y. Suetsugu, J. Byrd, C. M. Celata, J. Corlett, S. De Santis, M. Furman, A. Jackson,

- R. Kraft, D. Munson, G. Penn, D. Plate, A. Rawlins, M. Venturini, M. Zisman, D. Kharakh, M. Pivi, and L. Wang, *The conversion and operation of the cornell electron storage ring as a test accelerator (cesrta) for damping rings research and development*, Proceedings of the 2009 Particle Accelerator Conference, Vancouver, BC, 2009, pp. 4200–4204.
- [21] M. A. Palmer, M. G. Billing, R. E. Meller, M. C. Rendina, N. T. Rider, D. L. Rubin, J. Shanks, C. R. Strohman, and R. L. Holtzapple, *Cesr beam position monitor system upgrade for cesrta and chess operations*, Proceedings of the 2010 International Particle Accelerator Conference, Kyoto, Japan, ACFA, 2010, pp. 1191–1193.
- [22] M. A. Palmer, J. A. Crittenden, and J. Urban, *Design considerations and modeling results for ilc damping ring wigglers based on the cesr-c superconducting wiggler*, Proceedings of the 2007 Particle Accelerator Conference, Albuquerque, NM (C. Petit-Jean-Genaz, ed.), IEEE, 2007, pp. 3014–3016.
- [23] D. Rice, *Cesr-c: A wiggler-dominated collider*, Proceedings of the 2007 Particle Accelerator Conference, Albuquerque, NM (C. Petit-Jean-Genaz, ed.), IEEE, 2007, pp. 48–52.
- [24] D. Rice, S. Chapman, R. Gallagher, Y. He, J. Kandaswamy, V. Medjidzade, A. Mikhailichenko, N. Mistry, T. Moore, S. Richichi, K. Smolenski, A. B. Temnykh, W. Trask, and E. Smith, *Production and testing considerations for cesr-c wiggler magnets*, Proceedings of the 2003 Particle Accelerator Conference, Portland, OR (Joe Chew, Peter Lucas, and Sara Webber, eds.), IEEE, 2003, pp. 167–169.
- [25] J. Shanks, *Low-Emittance Tuning Techniques at CesrTA*, Proceedings of Low-Emittance Rings 2011 Workshop.
- [26] J. Shanks, D. L. Rubin, and D. Sagan, *Low-emittance tuning at the cornell electron storage ring test accelerator*, Phys. Rev. ST Accel. Beams **17** (2014).
- [27] S. T. Wang, D. L. Rubin, J. Conway, M. Palmer, D. Hartill, R. Campbell, and R. Holtzapple, *Visible-light beam size monitors using synchrotron radiation at cesr*, Nucl. Instrum. Methods Phys. Res. **A703** (2013), 80–90.